HHS Public Access

Author manuscript

Bioorg Med Chem Lett. Author manuscript; available in PMC 2017 January 01.

Published in final edited form as:

Bioorg Med Chem Lett. 2016 January 1; 26(1): 133–139. doi:10.1016/j.bmcl.2015.11.015.

Synthesis and evaluation of *N*-(methylthiophenyl)picolinamide derivatives as PET radioligands for metabotropic glutamate receptor subtype 4

Kun-Eek Kil[a], **Pekka Poutiainen**[a], **Zhaoda Zhang**[a], **Aijun Zhu**[a], **Darshini Kuruppu**[b], **Shilpa Prabhakar**[c], **Ji-Kyung Choi**[a], **Bakhos A. Tannous**[c], and **Anna-Liisa Brownell**[a,*]

[a]Athinoula A. Martinos Center for Biomedical Imaging, Department of Radiology, Massachusetts General Hospital, Charlestown, MA 02129, USA

[b]Department of Surgery, Massachusetts General Hospital, Boston, MA 02114, USA

[c]Experimental Therapeutics and Molecular Imaging Laboratory, Department of Neurology, Neuroscience Center, Massachusetts General Hospital, Boston, MA, 02114, USA

Abstract

In recent years, $mGlu_4$ has received great research attention because of the potential benefits of $mGlu_4$ activation in treating numerous brain disorders, such as Parkinson's disease (PD). A specific $mGlu_4$ PET radioligand could be an important tool in understanding the role of $mGlu_4$ in both healthy and disease conditions, and also for the development of new drugs. In this study, we synthesized four new *N*-(methylthiophenyl)picolinamide derivatives **11–14**. Of these ligands, **11** and **14** showed high *in vitro* binding affinity for $mGlu_4$ with IC_{50} values of 3.4 nM and 3.1 nM, respectively, and suitable physicochemical parameters. Compound **11** also showed enhanced metabolic stability and good selectivity to other mGluRs. [^{11}C]**11** and [^{11}C]**14** were radiolabeled using the [^{11}C]methylation of the thiophenol precursors **20a** and **20c** with [^{11}C]CH_3I in 19.0% and 34.8% radiochemical yields (RCY), and their specific activities at the end of synthesis (EOS) were 496 ± 138 GBq/μmol (n=6) and 463 ± 263 GBq/μmol (n=4), respectively. The PET studies showed that [^{11}C]**11** accumulated fast into the brain and had higher uptake, slower washout and 25% better contrast than [^{11}C]**2,** indicating improved imaging characteristics as PET radiotracer for $mGlu_4$ compared to [^{11}C]**2**. Therefore, [^{11}C]**11** will be a useful radioligand to investigate $mGlu_4$ in different biological applications.

Graphical Abstract

*For correspondence or reprints, contact: Anna-Liisa Brownell Athinoula A. Martinos Center for Biomedical Imaging 149, 13th St. Suite 2301 Charlestown, MA 02129, USA, abrownell@mgh.harvard.edu, Phone: 617-726-3807.

Notes

The authors declare no competing financial interest.

Supplementary material

Supplementary material (experimental procedures, spectroscopic characterization, HPLC data, *in vitro* selectivity data, and TACs for $mGlu_4$ blocking studies) associated with this article can be found in the online version.

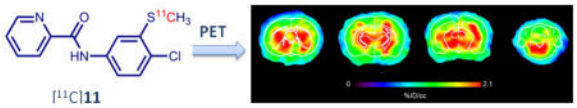

Keywords

PET; metabotropic glutamate receptor subtype 4 ($mGlu_4$); positive allosteric modulator (PAM)

As the most abundant excitatory neurotransmitter in the central nervous system (CNS) of vertebrates, L-glutamate mediates more than 50% of all synapses.[1, 2] Metabotropic glutamate receptors (mGluRs) and ionotropic glutamate receptors (iGluRs) are two major classes of glutamate receptors. The mGluRs belong to the class C G protein-coupled receptors (GPCR) superfamily, which have a distinct large extracellular N-terminus. The mGluRs can be further divided into three subgroups including eight known receptor subtypes (group I: $mGlu_1$ and $mGlu_5$, group II: $mGlu_2$ and $mGlu_3$, and group III: $mGlu_4$, $mGlu_6$, $mGlu_7$ and $mGlu_8$) based on their structural similarity, ligand specificity, and preferred coupling mechanisms.[3] The mGluRs have distinctive biodistribution in CNS depending on subtypes and subgroups and are involved in glutamate signaling in almost every excitatory synapse in CNS.[4]

In recent years, $mGlu_4$ has received a lot of research attention because of the potential benefits of $mGlu_4$ activation in treating several brain disorders, such as Parkinson's disease (PD).[5–7] As a group III mGluR, $mGlu_4$ interacts with the $G_{\alpha i/o}$ subunit of G-protein which negatively couples with adenylate cyclase to inhibit cAMP dependent signal pathways.[8, 9] The $mGlu_4$ is expressed at multiple synapses throughout the basal ganglia, mainly localized presynaptically and expressed in the striatum, hippocampus, thalamus, and cerebellum.[3, 10, 11] Its activation reduces neurotransmitter release, a mechanism implicated in the pathophysiology of PD. The activation of $mGlu_4$ can be accomplished by two different mechanisms: orthosteric agonists (competing with L-glutamate at the extracellular *N*-terminal's Venus Flytrap Domain) or noncompetitive positive allosteric modulators (PAMs). Previous orthosteric ligands of $mGlu_4$ lack clear subtype selectivity and blood-brain barrier (BBB) penetration. However, noteworthy examples of selective and brain penetrant orthosteric agonists such as LSP4-2022 exist.[12, 13]

Much recent effort has been focused on the development of allosteric modulators, which target the seven-transmembrane spanning domain. In particular, the allosteric modulation of $mGlu_4$ has prompted intense interest after (−)-PHCCC (**1**), a partially selective $mGlu_4$ PAM, was discovered and demonstrated activity in models of neuroprotection and PD.[14] There has been substantial progress in identifying PAMs for $mGlu_4$, and hundreds of $mGlu_4$ PAMs have been reported and/or patented since 2009.[5, 15, 16] Fig. 1 shows representative $mGlu_4$ PAMs.[5, 15, 17–20] Subsequent results with $mGlu_4$ PAMs have further validated the antiparkinsonian activity in animal models of PD.[11, 19, 21–24] This approach has opened a new avenue for developing nondopaminergic treatments for PD and for identifying novel disease modifying therapeutics.

As a noninvasive medical and molecular imaging technique and a powerful tool in neurological research, positron emission tomography (PET) offers a possibility to visualize and analyze the target receptor expression under physiological and pathophysiological conditions. PET has mostly been used to detect disease-related biochemical changes before the disease-associated anatomical changes can be found using standard medical imaging modalities. Moreover, PET radiotracers serve as invaluable biomarkers during the development of potential therapeutic drugs. Thus, extensive research effort has been directed towards the development of PET radioligands suitable for probing $mGlu_1$ and $mGlu_5$, in which many PET radiotracers have been reported and several of which, such as [^{18}F]FIMX[25] for $mGlu_1$, and [^{18}F]FPEB[26,27], [^{18}F]SP203[28] and [^{11}C]ABP688[29] for $mGlu_5$, have been advanced for human clinical trials.

Although many PET probes have been developed for $mGlu_1$ and $mGlu_5$, $mGlu_4$ still lacks useful PET radioligands for clinical study. A specific $mGlu_4$ PET radioligand could be an important tool for understanding the role of $mGlu_4$ in healthy and disease conditions, and also for the development of new drugs targeting this receptor. Recently, we reported a carbon-11 labeled PET radioligand [^{11}C]**2**[30] and a fluorine-18 labeled PET radioligand [^{18}F]**8**[31] (Fig. 2). These compounds exhibited some favorable features as PET radioligands such as fast uptake into the brain and specific accumulation in $mGlu_4$-rich regions of the brain. However, in comparison to one of the best $mGlu_5$ PET radiotracers [^{18}F]FPEB[26, 27], these compounds showed decreased retention time in the brain, which may affect the quality of imaging. The results indicate that the affinity and metabolic stability of this class of radiotracers need further optimization.

Thus, we have carried out the structure-affinity relationship (SAR) study of a series of new *N*-phenylpicolinamide derivatives.[32] It was then discovered that the 3-methylthio group was superior to the 3-methoxy group for $mGlu_4$ affinity by comparing compounds **9** (IC_{50}=13.7 nM) and **10** (IC_{50}=4.9 nM), showing a 2.8 fold enhancement in affinity. Metabolic stability was considered one of the major issues for ML128 (**2**), in which the 3-methoxy group was recognized as the metabolic soft group. As the *N*-methylthiophenyl derivatives may have a different metabolic profile from the corresponding *N*-methoxyphenyl analogs, it is interesting to understand its effect on the metabolic stability of the picolinamide derivatives. Based on these reasons, we extended our SAR study to four new *N*-(methylthiophenyl)picolinamide derivatives **11–14** (Fig. 3).

Compounds **11** and **12** have a Cl- or F-substitution at the 4-phenyl position, respectively, in which the same substitutions have enhanced the affinity for *N*-(3-methoxyphenyl)picolinamide and they may have a similar effect for *N*-(3-(methylthio)phenyl)picolinamide. The 4-phenyl position of the *N*-phenylpicolinamide was tolerated with a relatively large substitution as demonstrated in compounds **6** and **7**, so we synthesized compounds **13** and **14**, which are the regioisomers of **10** and **11**, respectively. Furthermore, these compounds can be easily radiolabeled by carbon-11 on the thiomethyl group.

Since poor BBB permeability and high nonspecific binding (NSB) are among the frequent causes for failure in CNS PET radioligand development, it is necessary to consider some

important physicochemical parameters such as MW, cLogP, tPSA, and HBD at the design stage. It has been proposed that more desirable ranges for CNS drugs are tPSA < 90; HBD < 3; 2 < cLogP < 5; and MW < 450.[33] As shown in Fig. 3, these compounds possess favorable physicochemical parameters, making them good candidates for CNS ligand development.

The syntheses of compounds **11–14** are illustrated in Scheme 1. Compounds **11** and **12** were synthesized in six steps (Scheme 1a). 5-Amino-2-halo-thiophenol (**17a** and **17b**) were prepared by the chlorosulfonylation of 4-halo-nitrobenzene (**15a** and **15b**) followed by tin(II) chloride mediated reduction in acidic media. To prevent nucleophilic attack on the thiol group during the amide coupling reaction, **17a** and **17b** were oxidized to form a disulfide bond. The resulting amino-dimer **18a** and **18b** were coupled with picolinic acid or its acid chloride under the corresponding amide coupling conditions to give **19a** and **19b**. The disulfide bond in **19a** and **19b** was reduced using either sodium borohydride or tris(2-carboxyethyl)phosphine hydrochloride (TCEP˙HCl) to give the corresponding thiophenol derivatives, **20a** and **20b**, respectively. **20a** and **20b** were methylated using iodomethane (CH_3I) in presence of potassium carbonate (K_2CO_3) or diisopropylethylamine (DIPEA) to give **11** and **12**, respectively. Compound **13** was synthesized by an amide coupling reaction between acid chloride of picolinic acid and aniline **21** in 60% yield (Scheme 1b). Compound **14** was synthesized from **22** in four steps. **22** was derivatized with ammonium thiocyanate to give **23** in 65% yield. Picolinic acid was converted to acid chloride and then coupled with **23** to form amide **24** in 88% yield. The nitrile group in **24** was removed by sodium borohydride to give **20c** in 75% yield. The methylation of **20c** was carried out using CH_3I and K_2CO_3 to give **14** in 28% yield (Scheme 1c).

Compounds, **2** and **9–14**, were evaluated with competitive binding studies using $mGlu_4$ transfected CHO cells by increasing the concentration of test materials from 0.01 nM to 10 μM in the presence of 2 nM of [^{3}H]**2**.[31] As shown in Table 1, the IC_{50} values of **11** and **14** are 3.4 and 3.1 nM, respectively, in which the affinity is enhanced by 1.5–1.6 fold compared to **2** (IC_{50} = 5.1 nM). Compound **10** (IC_{50} = 4.9 nM) has a similar affinity to **2**, while compounds **12** and **13** show reduced affinity. Compounds **10–14** were further tested for their metabolic stability in microsome from rat liver extract. Compound **2** was also examined at the same time as a reference. As Table 1 shows, the metabolic stabilities are in the following order: **11**>**2**>**10**>**12**>**13**>**14**. Although the half-life difference between compounds **2** and **11** is not significant, we anticipate that the difference of the half-life in the brain between these two compounds could be more significant. It is interesting to note that as the regioisomers of **10** and **11**, compounds **13** and **14** display a substantial decreased trend in metabolic stability. The results show that compound **11** has the most promising enhanced affinity and/or increased *in vitro* microsomal stability compared to other compounds (significance $p<0.05$, t-test) in this series.

The selectivity of **11** to other mGluRs including group I ($mGlu_1$ and $mGlu_5$), II ($mGlu_2$) and III ($mGlu_6$ and $mGlu_8$) were checked (Supplementary material). The assays were carried out at eight different concentrations between 0.1 nM and 30 μM of **11**. The results indicated that compound **11** did not have agonist and antagonist activities (>30 μM) toward $mGlu_1$, $mGlu_5$, $mGlu_2$ and $mGlu_6$, but displayed a weak agonist activity to $mGlu_8$ (EC_{50} = 14

μM).[34, 35] The selectivity data supports compound **11** as the most promising imaging agent candidate.

Since compounds **11** and **14** displayed the most promising affinity, they were selected for *in vivo* evaluation as potential $mGlu_4$ radiotracers and were compared to [^{11}C]**2** to understand how their structure, affinity, and metabolic stability affect PET imaging.

Carbon-11 labeling was performed by methylation of the thiophenol precursors (**20a** and **20c**) using [^{11}C]CH_3I and K_2CO_3 in acetone at 50 °C for 3 min (Scheme 2). All radiosyntheses took 35–40 min from the end of bombardment (EOB) to the end of synthesis (EOS). The carbon-11 labeled compounds [^{11}C]**11** and [^{11}C]**14** were obtained in 19.0 ± 7.7% (n=7) and 34.8 ± 8.0% (n=4) RCYs from [^{11}C]CO_2, respectively. Their specific activities were 496 ± 138 GBq/μmol (n=6) and 463 ± 263 GBq/μmol (n=4) at EOS, respectively.

Fig. 4a indicates that the difference in retention times between the precursors (**20a** and **20c**) and the corresponding radiolabeled products ([^{11}C]**11** and [^{11}C]**14**) was big enough to purify the radiotracers as a baseline separation. The HPLC profile of [^{11}C]**14** was similar to that of [^{11}C]**11**. The identities of [^{11}C]**11** and [^{11}C]**14** were confirmed by coinjection with the corresponding unlabled compound on a radio-HPLC. As shown in Fig. 4b, the retention time of [^{11}C]**11** was the same as that of coinjected nonradioactive standard **11**. The QC analysis of [^{11}C]**14** was also conducted in the same way. The radiochemical purities of [^{11}C]**11** and [^{11}C]**14** determined by radio-TLC were 98.0 ± 0.5% (n = 7), and 97.5 ± 1.0% (n = 4), respectively. Similar results were also observed in the radio-HPLC analyses.

We determined the $LogD_{7.4}$ values for [^{11}C]**11** and [^{11}C]**14** as 3.15 ± 0.04 (n = 4) and 3.00 ± 0.05 (n = 4) using octanol and phosphate buffered saline (PBS, pH7.4), which lie in the range normally considered favorable for a PET radioligand. The calculated cLogP values of **11** and **14** are both 3.63 (Fig. 3), which is higher than the experimental values.

PET imaging studies were conducted using male Sprague Dawley rats. The *in vivo* uptake and kinetics were examined using small-animal PET. The PET images (Fig. 5) indicated that [^{11}C]**11** and [^{11}C]**14** crossed the BBB quickly and were mainly accumulated in the thalamus, hippocampus, cerebellum, and striatum, which were reported as the $mGlu_4$-rich regions of the rat brain.[10, 36–38] We also acquired PET images of [^{11}C]**2** in the same time frames for comparison. To confirm the corresponding brain regions, anatomical templates of rat brains were used for the images with [^{11}C]**11** (Fig. 5). The results suggested that [^{11}C]**11** gave the best contrast among the three radiotracers and displayed better images in the hippocampus, striatum, thalamus and cerebellum. Using the $mGlu_4$-negligible region in the brain as a reference, we calculated the uptake ratio (contrast) of radioactivity between the $mGlu_4$-rich and the reference regions (areas immediately outside the cortical areas) from the reconstructed PET images. The maximum ratio was 1.67 ± 0.08 (n = 30; 10 images in 3 baseline studies) for [^{11}C]**2** and 2.10 ± 0.25 (n = 30) for [^{11}C]**11**. The results show that the signal to noise ratio of [^{11}C]**11** was enhanced up to 25% compared to [^{11}C]**2**.

The regional time-activity curves (TACs) of PET with [^{11}C]**2**, [^{11}C]**11**, and [^{11}C]**14** in the hippocampus, striatum, thalamus and cerebellum of rat brains are given in Fig. 6. The %ID/cc values at each time point obtained from the different PET images were averaged for each radiotracer and converted into TACs. As shown in the TACs, the radioactivity of [^{11}C]**2**, [^{11}C]**11**, and [^{11}C]**14** quickly increased in the brain within 2 min after a tail vein injection and then washed out within 20 min. The maximum radioactivity uptake depends on the region in the brain. The highest uptake for [^{11}C]**11** was seen in the thalamus, followed by the striatum, hippocampus, and cerebellum. The results indicate that [^{11}C]**11** has better brain uptake than [^{11}C]**2** and [^{11}C]**14** and is an improved PET radioligand for $mGlu_4$.

A blocking experiment for [^{11}C]**11** was carried out 2 h after the baseline scans to compare blocking images with baseline images. An $mGlu_4$ PAM (**3**·HCl) was used as an $mGlu_4$ blocking agent. The blocking agent was administered intravenously 1 min before [^{11}C]**11** injection.

The $mGlu_4$ blocking effects with compound **3** were 19–24% for first 5 min in selected regions of interest (ROIs). (Fig. 7) The incomplete blocking effect by compound **3** might be attributed to its relatively weak affinity and fast kinetics.[17,32]

In this study, we synthesized four new *N*-(methylthiophenyl)picolinamide derivatives **11–14**. Of these ligands, **11** and **14** showed high *in vitro* binding affinity for $mGlu_4$ together with suitable physicochemical parameters. Compound **11** also showed enhanced metabolic stability and good selectivity to other mGluRs. [^{11}C]**11** and [^{11}C]**14** were radiolabeled via the [^{11}C]methylation of the thiophenol precursors, **20a** and **20c**, with [^{11}C]CH_3I in reliable RCYs and specific activities. The PET studies showed that [^{11}C]**11** accumulated fast into the brain and had higher uptake, slower washout and 25% better contrast than [^{11}C]**2,** indicating improved imaging characteristics as a PET radiotracer for $mGlu_4$ compared to [^{11}C]**2**. [^{11}C]**11** will be a useful radioligand to investigate $mGlu_4$ in different biological applications.

Supplementary Material

Refer to Web version on PubMed Central for supplementary material.

Acknowledgments

Funding Sources

NIBIB-R01EB012864 and NIMH-R01MH91684 to A-L Brownell.

The authors would like to thank the technical support of the PET/MRI and radiochemistry facility at the Athinoula A. Martinos Center for Biomedical Imaging at Massachusetts General Hospital for the operation of cyclotron and synthesis modules. The authors are also grateful to Drs. Tanabe and Nakanishi's laboratory (Osaka Bioscience Institute, Osaka, Japan) for providing the vector of mGlu4 from the rat as a gift. The following supporting instrument grants (1S10RR029495-01, 1S10RR026666-01, and 1S10RR023452-01) are also appreciated. The authors appreciate the generous help of the NIMH PDSP program (Contract # HHSN-271-2008-00025-C) led by Dr. Bryan L. Roth MD, PhD at the University of North Carolina at Chapel Hill and the Project Officer Jamie Driscol at NIMH, Bethesda MD, USA. Finally, the authors would like to express their appreciation of the financial support for PP from The Orion Farmos Research Foundation, Saastamoinen Foundation, Sigrid Juselius Foundation, Osk Huttunen Foundation and Kuopio University Foundation.

References and notes

1. Conn PJ. Ann N Y Acad Sci. 2003; 1003:12. [PubMed: 14684432]
2. Watkins JC, Jane DE. Br J Pharmacol. 2006; 147:S100. [PubMed: 16402093]
3. Conn PJ, Pin JP. Annu Rev Pharmacol Toxicol. 1997; 37:205. [PubMed: 9131252]
4. Riedel G, Platt B, Micheau J. Behav Brain Res. 2003; 140:1. [PubMed: 12644276]
5. Robichaud AJ, Enger DW, Lindsley CW, Hopkins CR. ACS Chem Neurosci. 2011; 17:433. [PubMed: 22860170]
6. Amalric M, Lopez S, Goudet C, Fisone G, Battaglia G, Nicoletti F, Pin JP, Acher FC. Neuropharmacol. 2013; 66:53.
7. Huang X, Dale E, Brodbeck RM, Doller D. Curr Top Med Chem. 2014; 14:1755. [PubMed: 25183417]
8. Fettagutti F, Balani-Guerra B, Corsi M, Nakanishi S, Corti C. Eur J Neurosci. 1999; 11:2073. [PubMed: 10336676]
9. Niswender CM, Conn PJ. Annu Rev Pharmacol Toxicol. 2010; 50:295. [PubMed: 20055706]
10. Corti C, Aldegheri L, Somogyi P, Ferraguti F. Neuroscience. 2002; 110:403. [PubMed: 11906782]
11. Valenti O, Mannaioni G, Seabrook GR, Conn PJ, Marino MJ. J Pharmcol Exp Ther. 2005; 313:1296.
12. Goudet C, Vilar B, Courtiol T, Deltheil T, Bessiron T, Brabet I, Oueslati N, Rigault D, Bertrand HO, McLean H, Daniel H, Amalric M, Acher F, Pin JP. FASEB J. 2012; 26:1682. [PubMed: 22223752]
13. Cajina M, Nattini M, Song D, Smagin G, Jørgensen EB, Chandrasena G, Bundgaard C, Toft DB, Huang X, Acher F, Doller D. ACS Med Chem Lett. 2014; 5:119. [PubMed: 24900783]
14. Marino MJ, Valenti O, Conn PJ. Drug & Aging. 2003; 20:377.
15. Lindsley CW, Hopkins CR. Expert Opin Ther Pat. 2012; 22:461. [PubMed: 22506633]
16. Zhang, Z.; Brownell, A-L. Neuroimaging - clinical applications. Bright, P., editor. Intech; Rijeka, Croatia: 2012. p. 499
17. Engers DW, Niswender CM, Weaver CD, Jadhav S, Menon UN, Zamorano R, Conn PJ, Lindsley CW, Hopkins CR. J Med Chem. 2009; 52:4115. [PubMed: 19469556]
18. Kalinichev M, Le Paul E, Boléa C, Girard F, Campo B, Fonsi M, Royer-Urios I, Browne SE, Uslaner JM, Davis MJ, Raber J, Duvoisin R, Bate ST, Reynolds IJ, Poli S, Celanire S. J Pharmacol Exp Ther. 2014; 350:495. [PubMed: 24947466]
19. Le Poul E, Bolea C, Girard F, Poli S, Charvin D, Campo B, Bortoli J, Bessif A, Luo B, Koser AJ, Hodge LM, Smith KM, DiLella AG, Liverton N, Hess F, Browne SE, Reymonds IJ. J Parmacol Exp Ther. 2012; 343:167.
20. Hong SP, Liu KG, Ma G, Sabio M, Uberti MA, Bacolod MD, Peterson J, Zou ZZ, Robichaud AJ, Doller D. J Med Chem. 2011; 54:5070. [PubMed: 21688779]
21. Jones CK, Engers DW, Thompson AD, Field JR, Blobaum AL, Lindsley SR, Zhou Y, Gogliotti RD, Jadhav S, Zamorano R, Bogenpohl J, Smith Y, Morrison R, Daniels JS, Weaver CD, Conn PJ, Lindsley CW, Niswender CM, Hopkins CR. J Med Chem. 2011; 54:7639. [PubMed: 21966889]
22. Valenti O, Marino MJ, Wittmann M, Lis E, DiLella AG, Kinney GG, Conn PJ. J Neurosci. 2003; 23:7218. [PubMed: 12904482]
23. Bennouar K-E, Uberti MA, Melon C, Bacolod MD, Jimenez HN, Cajina M, Kerkerian-Le Goff L, Doller D, Gubellini P. Neuropharmacol. 2013; 66:158.
24. Iderberg H, Maslava N, Thompson AD, Bubser M, Niswender CM, Hopkins CR, Lindsley CW, Conn PJ, Jones CK, Cenci MA. Neuropharmacol. 2015; 95:121.
25. Xu R, Zanotti-Fregonara P, Zoghbi SS, Gladding RL, Woock AE, Innis RB, Pike VW. J Med Chem. 2013; 56:9146. [PubMed: 24147864]
26. Patel S, Hamill T, Connolly B, Jagoda E, Li W, Gibson R. Nucl Med Biol. 2007; 34:1009. [PubMed: 17998106]
27. Wang J, Tueckmantel W, Zhu A, Pellegrino D, Brownell AL. Synapse. 2007; 61:951. [PubMed: 17787003]

28. Brown A, Kimura Y, Zoghbi SS, Siméon FG, Liow JS, Kreisl WC, Taku A, Fujita M, Pike VW, Innis RB. J Nucl Med. 2008; 49:2042. [PubMed: 19038998]
29. Ametamey SM, Treyer V, Streffer J, Wyss MT, Schmidt M, Blagoev M, Hintermann S, Auberson Y, Gasparini F, Fischer UC, Buck A. J Nucl Med. 2007; 48:247. [PubMed: 17268022]
30. Kil KE, Zhang Z, Jokivarsi K, Gong C, Choi JK, Kura S, Brownell AL. Bioorg Med Chem. 2013; 21:5955. [PubMed: 23978356]
31. Kil K-E, Poutiainen P, Zhang Z, Zhu A, Choi J-K, Jokivarsi K, Brownell A-L. J Med Chem. 2014; 57:9130. [PubMed: 25330258]
32. Zhang Z, Kil KE, Poutiainen P, Choi JK, Kang HJ, Huang XP, Roth BL, Brownell AL. Bioorg Med Chem Lett. 2015; 25:3956. [PubMed: 26231155]
33. Hitchcock SA. Curr Opin Chem Biol. 2008; 12:318. [PubMed: 18435937]
34. Roth, BL. National Institute of Mental Health Psychoactive Drug Screening Program Assay Protocol Book. http://pdsp.med.unc.edu/PDSP%20Protocols%20II%202013-03-28.pdf
35. Shi Q, Savage JE, Hufeisen SJ, Rauser L, Grajkowska E, Ernsberger P, Wroblewski JT, Nadeau JH, Roth BL. J Pharmacol Exp Ther. 2003; 305:131. [PubMed: 12649361]
36. Bradley SR, Standaert DG, Rhodes KJ, Rees HD, Testa CM, Levey AI, Conn PJ. J Comp Neurol. 1999; 407:33. [PubMed: 10213186]
37. Kinoshita A, Ohishi H, Nomura S, Shigemoto R, Nakanishi S, Mizuno N. Neurosci Lett. 1996; 207:199. [PubMed: 8728484]
38. Lavreysen H, Dautzenberg FM. Curr Med Chem. 2008; 15:671. [PubMed: 18336281]

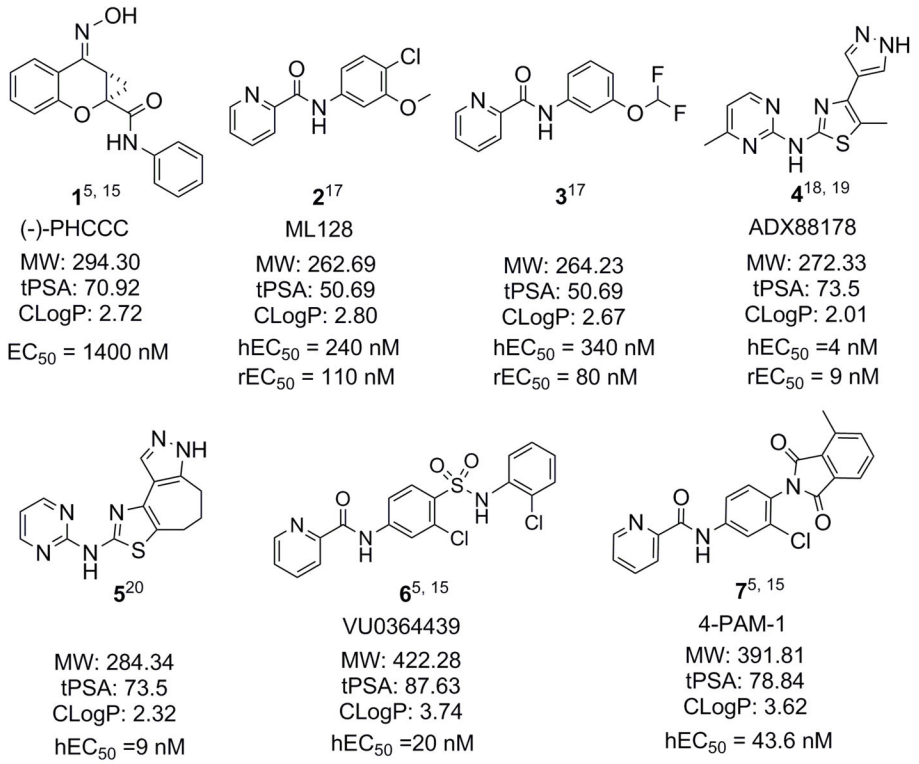

Figure 1.
Representative $mGlu_4$ PAMs.

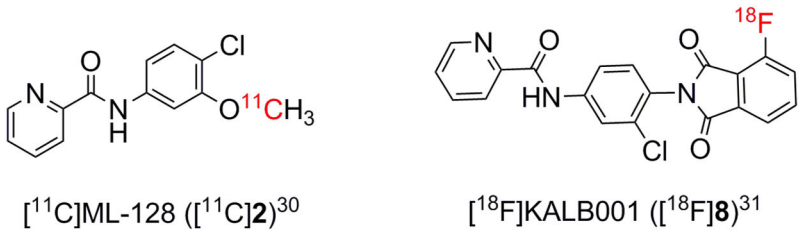

[^{11}C]ML-128 ([^{11}C]**2**)[30] [^{18}F]KALB001 ([^{18}F]**8**)[31]

Figure 2.
The PET radiotracers for $mGlu_4$.

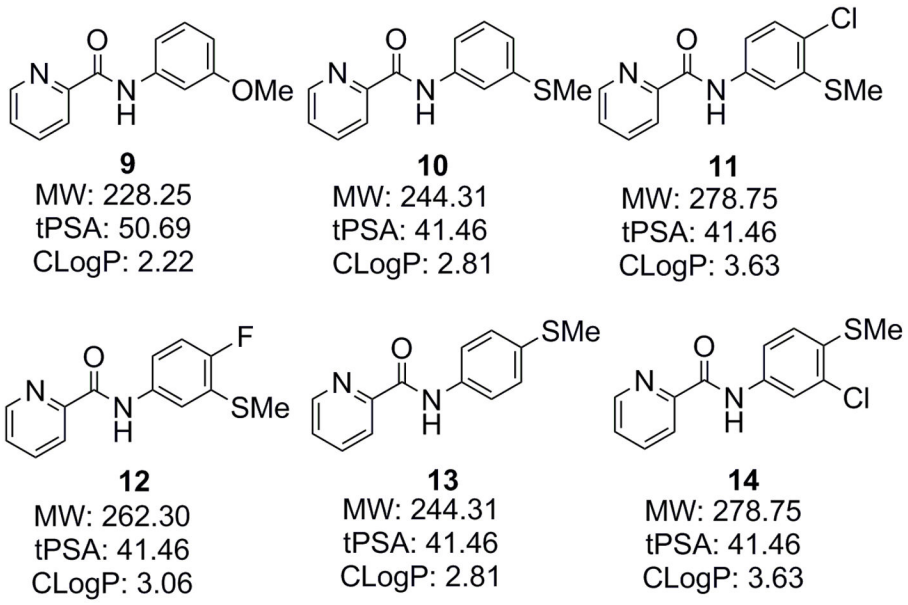

Figure 3.
The *N*-phenylpicoliamide derivatives for SAR study.

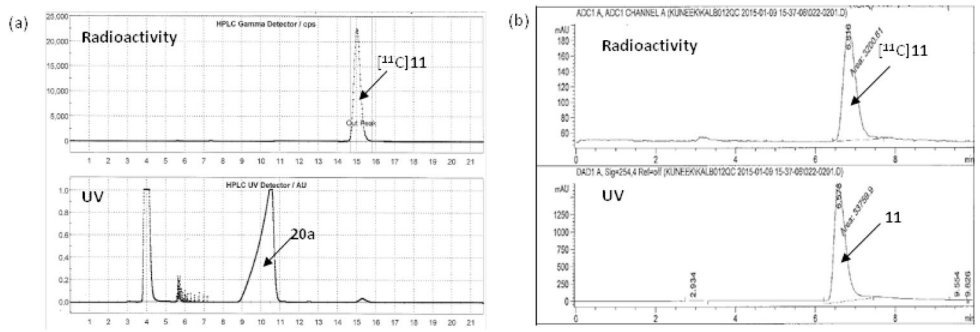

Figure 4.

The UV and radioactivity profiles (a) the reaction mixture was purified by a semi-preparative HPLC and (b) the QC analysis of the purified [^{11}C]**11** was carried out by an analytical HPLC. (a) Gemini-NX C_{18} semi-preparative column (Phenomenex, 250 mm × 10 mm, 5 μm), ammonium formate solution (0.1 M) : acetonitrile = 40:60, 4 mL/min (b) Alltima C_{18} analytical column (150 mm × 4.6 mm, 5 μm), 0.1% TFA solution : acetonitrile = 35:65, 1 mL/min.

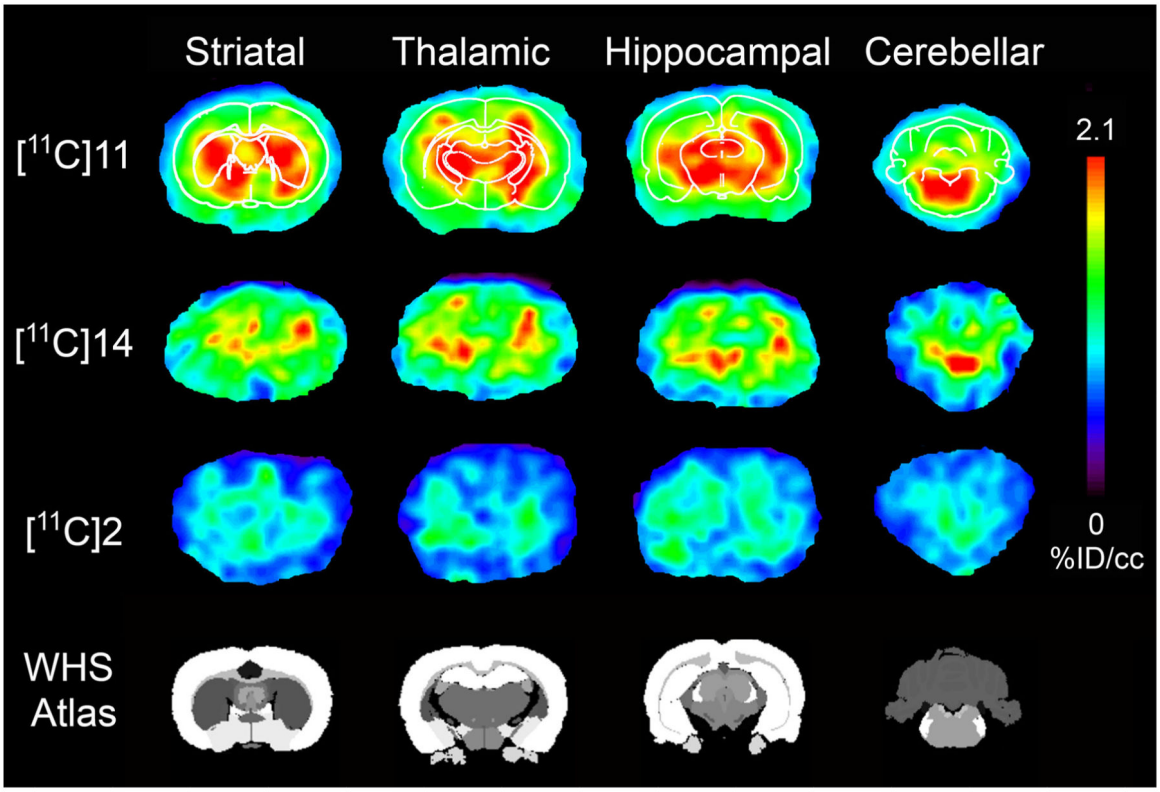

Figure 5.

Color-coded PET images of [^{11}C]**11**, [^{11}C]**14**, and [^{11}C]**2** at different brain levels (striatum, thalamus, hippocampus, and cerebellum). The images represent distribution of radioligand from 5 to 10 min after administration. All the images were normalized to the highest voxel value (%ID/cm^3) of the whole data set. These images demonstrate improved imaging characteristics of [^{11}C]**11** compared to [^{11}C]**14** and [^{11}C]**2** based on the high accumulation and slow washout. The thickness of each slice was 0.625 mm.

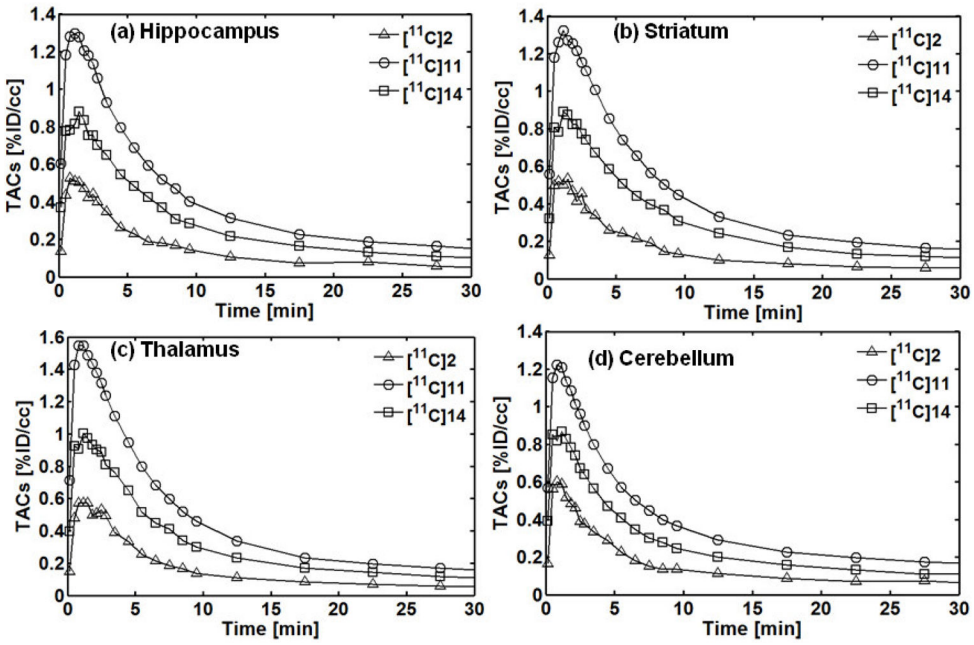

Figure 6.

Brain regional TACs of PET with [^{11}C]**2**, [^{11}C]**11**, and [^{11}C]**14** in (a) hippocampus, (b) striatum, (c) thalamus and (d) cerebellum of rat brain. The %ID/cc values at each time point were averaged from different studies for constructing TACs.

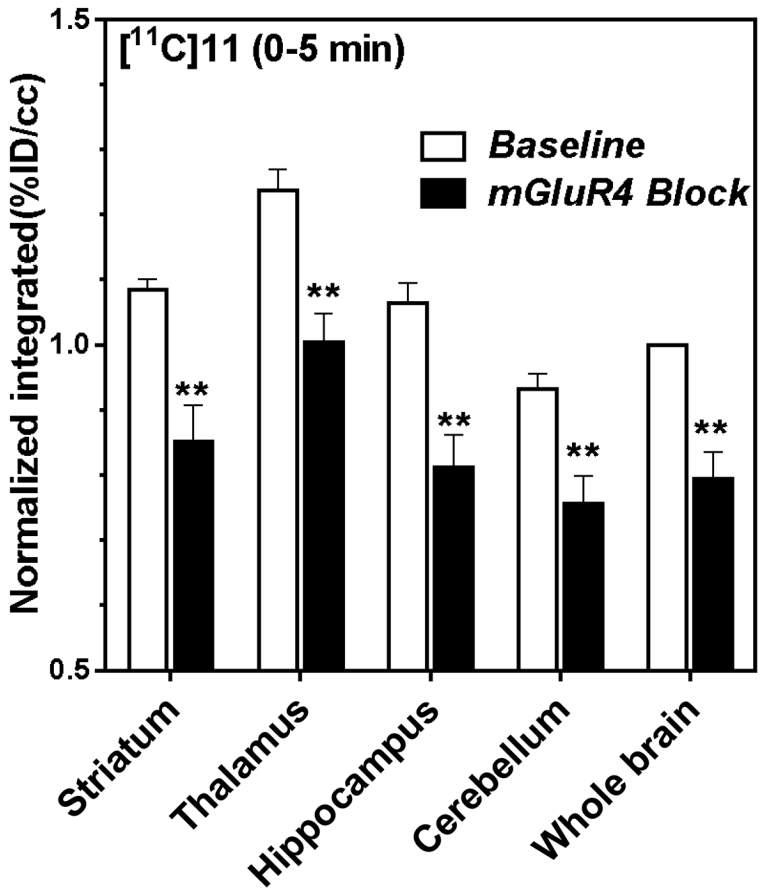

Figure 7.

Blocking studies of [^{11}C]**11** with an $mGlu_4$ PAM (**3**·HCl, 10 mg/kg, iv) during first 5 min after injection of [^{11}C]**11**. Each rat was scanned for baseline and individually normalized (whole brain was set as 1.0). The blocking study was done with same instrumentation and settings. The blocking results were normalized to corresponding baseline results. Integrals were calculated over 0–5 min time periods. (n=4 blotted with S.D and significances were calculated using t-test, ** = $p<0.01$)

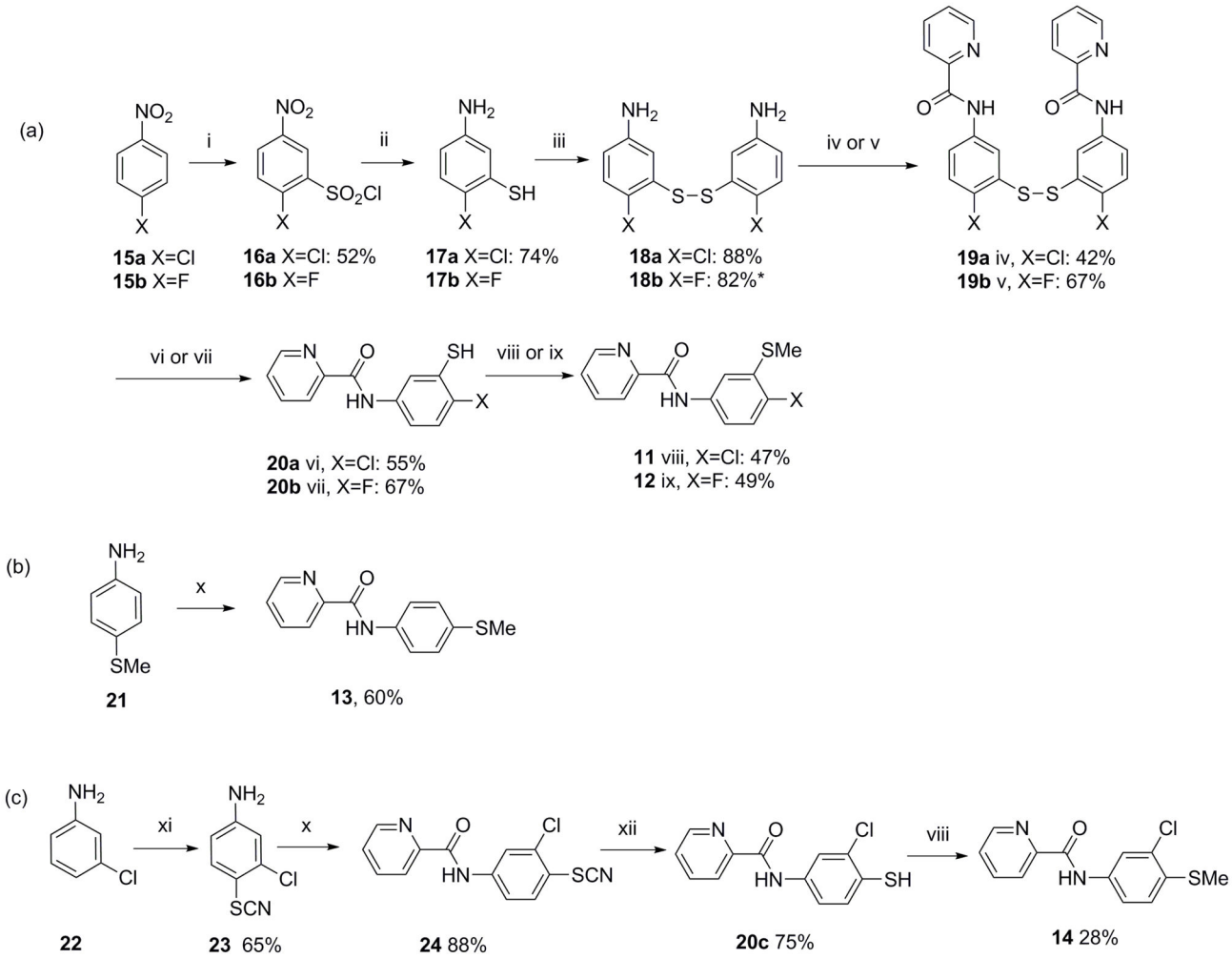

(i) $ClSO_3H$, 120°C (ii) $SnCl_2$, HCl, reflux (iii) DMSO, 80°C (iv) EDC.HCl, DIPEA, HOBt, Dioxane, 50°C, (v) Picolyl chloride, DIPEA, DMF, rt (vi) $NaBH_4$, EtOH, refux (vii) TCEP.HCl, DMF, rt (viii) K_2CO_3, Cs_2CO_3, MeI, rt (ix) DIPEA, MeI, CH_2Cl_2, rt (x) 1. Picolinic acid, $SOCl_2$, Benzene, reflux 2. TEA, THF, 40°C (xi) NH_4SCN, I_2, MeOH, rt (xii) $NaBH_4$, Erythritol, MeOH, 0°C; (*) Yield was based on **15b**.

Scheme 1.

Syntheses of **11–14** and thiophenol precursors, **20a** and **20c**.

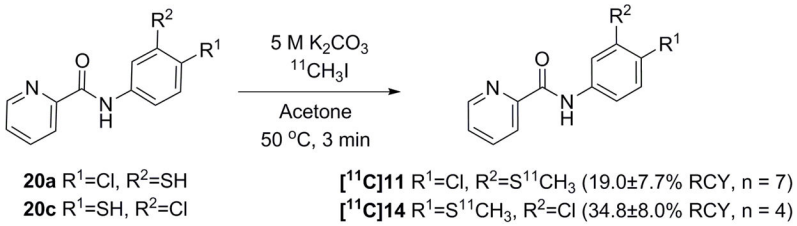

Scheme 2.

Radiosyntheses of [^{11}C]**11** and [^{11}C]**14**.

Table 1

In vitro properties.

	Affinity[a]		*Stability*[b]		
	IC_{50} (nM)	**Log(IC_{50} ± SEM)**	**$T_{1/2}$ (min)**	**κ[c] (min^{-1})**	**SEM(κ)**
2 (ML 128)	5.1	−8.29 ± 0.09[e]	5.99	0.116	0.007
9	13.7	−7.86 ± 0.10[e]	n.d.[d]	n.d.	n.d.
10	4.9	−8.31 ± 0.07[e]	5.83	0.119	0.009
11	3.4	−8.46 ± 0.07	6.54	0.106	0.005
12	7.8	−8.11 ± 0.10	5.73	0.121	0.008
13	13.3	−7.88 ± 0.09	4.14	0.168	0.013
14	3.1	−8.50 ± 0.09	3.86	0.179	0.016

[a] Binding inhibition assay

[b] Microsomal stability assay (rat)

[c] The decay constant that is slope of log concentration vs time profile ($t_{1/2}=\ln 2/\kappa$).

[d] Not determined

[e] Ref. 32

Bioorg Med Chem Lett. Author manuscript; available in PMC 2017 January 01.